



A quantum chemical study on a set of non-imidazole H₃ antihistamine molecules

Edson Barbosa da Costa, Milan Trsic*

Instituto de Química de São Carlos, Universidade de São Paulo, CP 780, 13560-970 São Carlos, São Paulo, Brazil

ARTICLE INFO

Article history:

Received 28 September 2009

Accepted 9 January 2010

Available online 18 January 2010

Keywords:

Molecular orbitals

QSAR

Antihistamine

H₃ receptor

Non-imidazole compounds

ABSTRACT

Molecular orbital calculations were carried out on a set of 28 non-imidazole H₃ antihistamine compounds using the Hartree–Fock method in order to investigate the possible relationships between electronic structural properties and binding affinity for H₃ receptors (pK_i). It was observed that the frontier effective-for-reaction molecular orbital (FERMO) energies were better correlated with pK_i values than highest occupied molecular orbital (HOMO) and lowest unoccupied molecular orbital (LUMO) energy values. Exploratory data analysis through hierarchical cluster (HCA) and principal component analysis (PCA) showed a separation of the compounds in two sets, one grouping the molecules with high pK_i values, the other gathering low pK_i value compounds. This separation was obtained with the use of the following descriptors: FERMO energies (ϵ_{FERMO}), charges derived from the electrostatic potential on the nitrogen atom (N¹), electronic density indexes for FERMO on the N¹ atom ($\sum_{(\text{FERMO})} c_i^2$), and electrophilicity (ω'). These electronic descriptors were used to construct a quantitative structure–activity relationship (QSAR) model through the partial least-squares (PLS) method with three principal components. This model generated $Q^2 = 0.88$ and $R^2 = 0.927$ values obtained from a training set and external validation of 23 and 5 molecules, respectively. After the analysis of the PLS regression equation and the values for the selected electronic descriptors, it is suggested that high values of FERMO energies and of $\sum_{(\text{FERMO})} c_i^2$, together with low values of electrophilicity and pronounced negative charges on N¹ appear as desirable properties for the conception of new molecules which might have high binding affinity.

© 2010 Elsevier Inc. All rights reserved.

1. Introduction

Arrang et al. discovered the histamine H₃ receptors in 1983 [1]. Autoradiographic studies showed that in the human brain H₃ receptors are predominantly located in areas associated with cognition, i.e., hippocampus, basal ganglia and cortical center [2]. In these regions, the neurotransmitter histamine associates with other amines synthesized by the human organism (acetylcholine, dopamine, noradrenaline and serotonin) which control some (patho)physiological processes [3]. Investigating the role of the histamine neurotransmitter, it was found that it inhibits its own release [4] and synthesis [5] in the central nervous system (CNS), via interaction with H₃ receptors; histamine also modulates the release of other neurotransmitters [6]. Because of these functions, research into the development of new substances (antagonists) that present inverse performance, has increased, mainly on account of their therapeutic applications in a number of CNS disorders [2,3], such as deficits in learning and memory, Alzheimer's disease, epilepsy, sleep disorders and obesity.

Since the 1980s, efforts have been directed towards the discovery of potent H₃ antagonist ligands. The main structural feature of the first class of ligands was the imidazole ring, which is inherent to histamine, connected to a polar group and a lipophilic residue. However, substances that have the imidazole ring in their structure present an undesirable potential metabolic liability [7–8]. In view of this fact, it is important to identify ligands without this inconvenience, and the latest discoveries of some compounds without the imidazole ring represent a breakthrough in this search. Recent studies [9] show that the number of patents for non-imidazole compounds has overtaken the number of those for compounds with the imidazole ring. This is an indication of the importance of experimental and theoretical studies of this class of compounds in the development of new H₃ receptor antagonists.

A pharmacophore model that has been used in the field of non-imidazole H₃ ligands has the following structural characteristics: (1) two basic character nitrogen atoms, (2) an aromatic ring, and (3) a polar group adjacent to the aromatic ring. A group of compounds that display these characteristics is shown in the general structure represented in Fig. 1(a), which led to the discovery of a potent antagonist (see Fig. 1(b)) [10]. Recently, Dvorak et al. [11] performed a structure activity relationship (SAR) study of two series of antihistamine H₃, with structures similar to the pharmacophore model shown in Fig. 1(a). This study was

* Corresponding author. Tel.: +55 16 3373 8032; fax: +55 16 3373 9982.
E-mail address: cra61@iqsc.usp.br (M. Trsic).

Table 2Chemical structures of 4-hydroxypiperidines used in the present investigation (group II) and their binding affinities for the human H₃ receptor (pK_i).

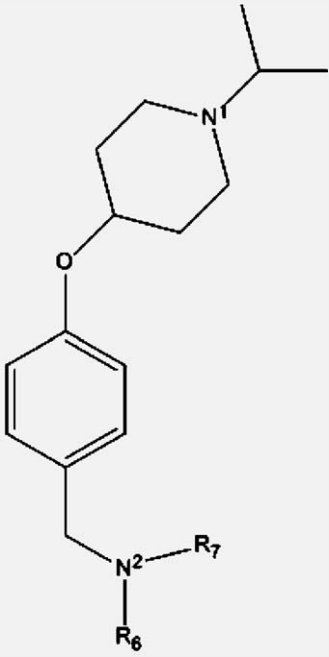
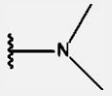
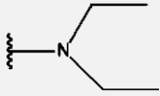
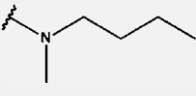
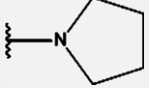
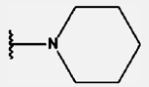
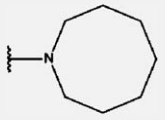
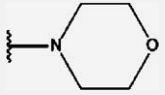
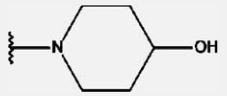
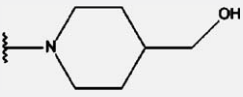
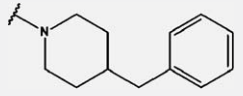
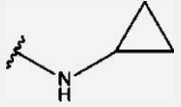
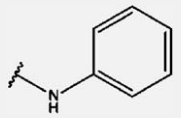
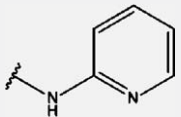
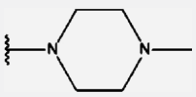
Basic structure of group II	Number	N ² R ₆ R ₇	pK _i
	11		8.52
	12		8.91
	13		8.83
	14		8.71
	15		9.20
	16		8.77
	17		8.67
	18		8.85
	19		9.00
	20		8.84
	21		8.79
	22		8.26
	23		8.65
	24		9.13

Table 2 (Continued)

Basic structure of group II	Number	$N^2R_6R_7$	pK_i
	25		8.70
	26		8.70
	27		9.00
	28		8.94

This descriptor seems significant as a result of the observation by Apodaca et al. [27] that the loss of the nitrogen atom severely reduces the pK_i value, as illustrated in Fig. 3.

- (b) Dipole moment (DM). The purpose for considering this descriptor is to evaluate whether the H_3 receptors favor the binding with polar molecules or, alternatively, with non-polar molecules.
- (c) Isotropic first order polarizability (α) [28]. The value of α indicates the facility with which the molecule would create an induced dipole due to the vicinity of other structures; this could be related to the ability to react with amino acids.
- (d) Hyperpolarizability or second order polarizability (β) [28]. This property is related to the electrophilic character of a molecule, that is, the larger the value of β , the greater the molecule's capacity to receive electrons.
- (e) The molecular volume (V). This is relevant when estimating steric effects in the H_3 antagonists.
- (f) The energies of the frontier orbitals HOMO (ϵ_{HOMO}) and LUMO (ϵ_{LUMO}). These descriptors are related to the electron donating or accepting character of a given compound [29–31].
- (g) The energies of the FERMOs (ϵ_{FERMO}). For the 28 molecules studied, the N^1 atom was selected as the reactive center, for the same reason that its charge was chosen as an important

parameter, as explained in item (a) above. The particular choice of FERMO for some molecules is shown in Fig. 4. It is remarkable the extent to which FERMO showed the best behavior, not necessarily corresponding to the same orbital for each of the molecules. This is shown in Fig. 4 for four orbitals. In this figure we can observe that FERMO has the same shape in each case, coinciding alternatively with HOMO₋₁ for the first two molecules, HOMO₋₂ for the third, and HOMO₋₃ for the forth. In Fig. 5, the energy correlation diagram for the same molecules is shown.

- (h) Electronic density indexes for HOMO ($\sum_{(HOMO)} c_i^2$), LUMO ($\sum_{(LUMO)} c_i^2$), and FERMO ($\sum_{(FERMO)} c_i^2$) for the N^1 atom. The summation is for the coefficients (c_i) of the atomic orbitals of the respective MO. This kind of index was used successfully by Subramanian et al. [32] in a quantum chemical and chemometric study of the activity of lapachol and some derivatives of 1,4-naphthoquinones against carcinosarcoma Walker 256, showing satisfactory performance as electronic descriptors.
- (i) Absolute softness (S), absolute hardness (η), electronic chemical potential (μ), absolute electronegativity (χ), and electrophilicity indexes (ω) were also calculated. The calculation of these indexes employs five different equations [33,34] that have ϵ_{HOMO} and ϵ_{LUMO} as variables, e.g., $\mu = (\epsilon_{LUMO} - \epsilon_{HOMO})/2$.

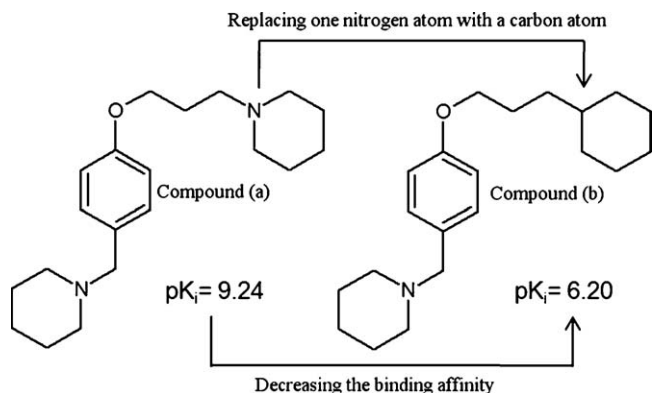


Fig. 3. Apodaca and collaborators [27] confirmed a decrease in binding affinity values for the H_3 receptor when one nitrogen atom is replaced by a carbon atom in 1-[4-(3-piperidin-1-ylpropoxy)benzyl]piperidine, compound (a), producing compound (b), 1-[4-(3-cyclohexylpropoxy)benzyl]piperidine. The study of compounds (a) and (b) with their binding affinity values and chemical structures are presented in Ref. [27].

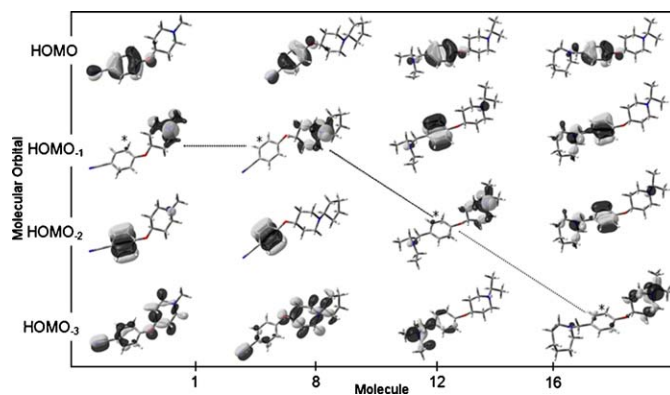


Fig. 4. The shapes of the highest occupied molecular orbital for four molecules: 1, 8, 12, and 16; for the numeration of the molecules see Tables 1 and 2. *Indicates the FERMO. Similar trends for molecular orbitals are confirmed for the other 24 molecules.

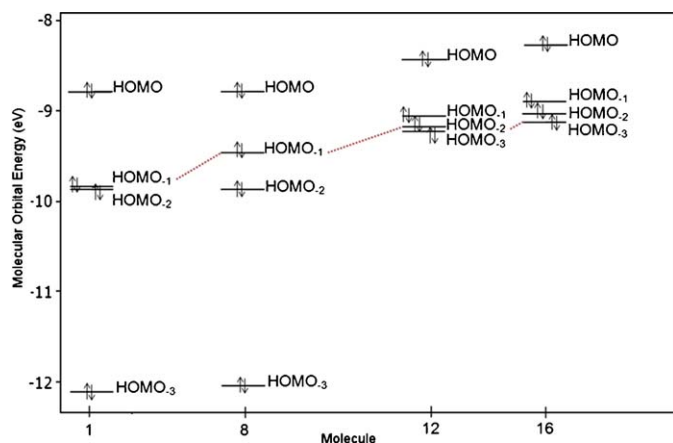


Fig. 5. Molecular orbital energy level diagram for molecules 1, 8, 12, and 16 showing the correlation between the FERMOs which are connected by dashed lines.

- (j) The former indexes S , η , μ , χ , ω were recalculated using the FERMO energies, instead of the HOMO energies, generating new reactivity indexes labeled as S' , η' , μ' , χ' , ω' . This strategy was partially employed by Da Silva et al. [35] to explain the behavior of some acids and bases with more than one reaction center using Person's hardness and softness indexes [33].

3. Results and discussion

3.1. Statistical analysis for correlation with pK_i

Linear correlation between the MO energies and the pK_i values is reported through the regression parameters shown in Table 3. Evaluating the statistical significance of the linear model, Fisher's F -value should have at least 10 times the value of the Fisher statistical test ($F_{(1,26)} = 9.41$, 99.9% confidence level) [36]. One can confirm that the energy of FERMO is better correlated with the pK_i measurements, since the F -value obtained is 139.47, more than 10 times the acceptable value, while for HOMO and LUMO values were 22.00 and 68.88, respectively. In addition, the regression employing the ϵ_{FERMO} energies presents the lowest standard deviation, 0.447, the lowest pK_i error, 0.200, and the square of the correlation coefficient (R^2) is 0.843. Thus, the second type of quantum indexes S' , η' , μ' , χ' , ω' , and $\sum_{(\text{FERMO})} c_i^2$ were chosen to assist in the selection of variables responsible for influencing the binding affinity.

The set of pre-selected properties (ϵ_{FERMO} , S' , η' , μ' , χ' , ω' , and $\sum_{(\text{FERMO})} c_i^2$) together with DM, α , β , V , and charges on the N^1 nitrogen atom were analyzed by multivariate methods [37], PCA and HCA. The descriptors ϵ_{FERMO} , N^1 charge, $\sum_{(\text{FERMO})} c_i^2$, and ω' appear to be the basis of a relevant separation of the compounds in two groups.

The PCA analysis shows that the three first principal components, PC1, PC2 and PC3 appear as significant and explain 98.3% of the total variance. Scores and loadings for the first two

Table 3

Linear regression parameters for pK_i values vs. LUMO, HOMO and FERMO energies as calculated with HF/6-31G(d,p).

Orbital	R^{2a}	pK_i erro	s^b	F^c	$F_{(1,26)}^d$
LUMO	0.726	0.348	0.590	68.88	9.41
HOMO	0.461	0.686	0.828	22.00	
FERMO	0.843	0.200	0.447	139.47	

^a The square of the correlation coefficient.

^b Standard deviation.

^c The Fisher F -value of the linear regression.

^d The statistical Fisher test (99% reliability level).

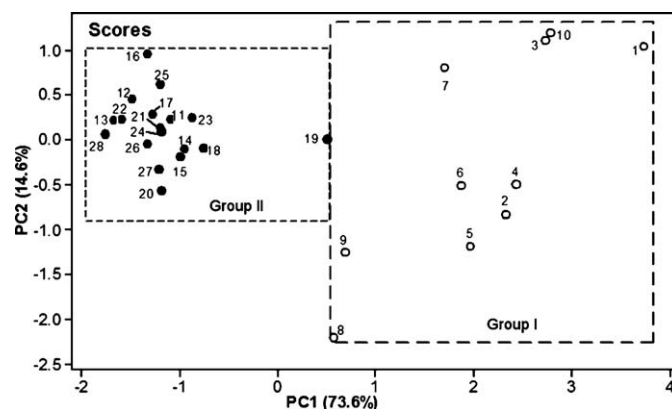


Fig. 6. Scores plot of PC2 against PC1 for the 28 compounds. Group II compounds are located on the left side, and group I compounds on the right side.

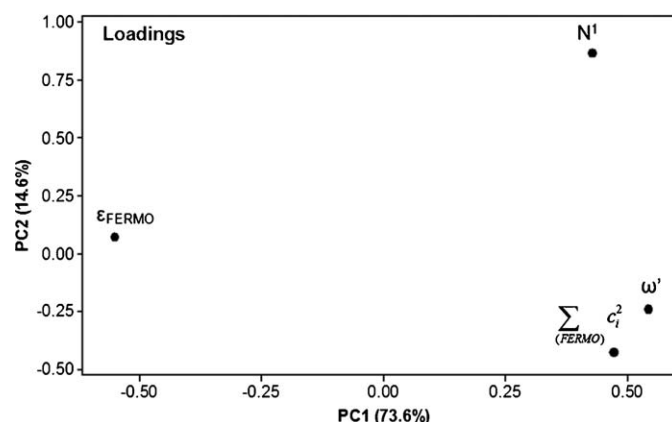


Fig. 7. PC1–PC2 loadings plot using the four descriptors indicated in Section 3.1.

components are presented in Figs. 6 and 7. The HCA dendrogram produced by the HCA analysis is exhibited in Fig. 8.

Fig. 6 indicates a clear distinction between two groups of compounds: ligands with lower binding affinity values (compounds 1–10) are grouped on the right-hand side, while those with higher binding affinity values (compounds 11–28) are located on the left side. In addition, as a complement to the former observation, in Fig. 7 for the loadings it is confirmed that the compounds with higher binding affinity values, located on the left side present a contribution of the ϵ_{FERMO} descriptor, situated on the

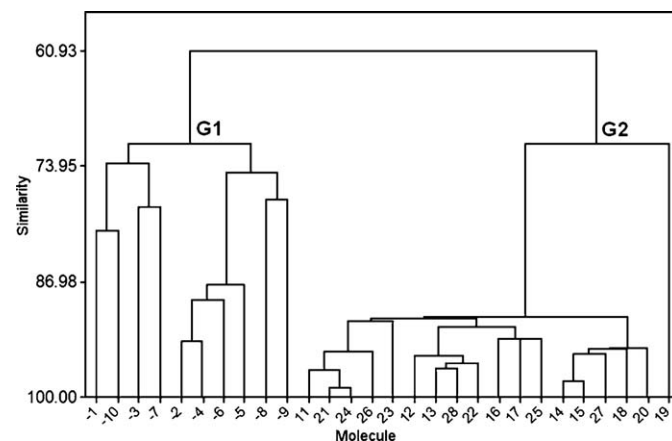


Fig. 8. HCA dendrogram with the high binding affinity compounds (with no sign) and the low binding affinity compounds (with negative signs). G1 and G2 are the clusters.

Table 4

The selected quantum chemical descriptors for the 28 compounds.

Group	Compound	pK_i	Quantum chemical descriptors			
			$\varepsilon_{\text{FERMO}}$ (eV)	N^1 charge (a.u.)	ω' (eV)	$\sum_{(\text{FERMO})} c_i^2$
I	1	5.37	−9.836	−0.512	0.468	0.508
	2	7.09	−9.571	−0.635	0.439	0.526
	3	6.97	−9.495	−0.514	0.431	0.516
	4	7.55	−9.564	−0.613	0.437	0.525
	5	6.12	−9.587	−0.671	0.444	0.516
	6	7.82	−9.481	−0.629	0.429	0.516
	7	7.18	−9.292	−0.551	0.411	0.511
	8	7.89	−9.469	−0.768	0.431	0.499
	9	7.49	−9.345	−0.702	0.418	0.503
	10	5.27	−9.697	−0.530	0.450	0.490
II	11	8.52	−9.144	−0.665	0.257	0.478
	12	8.91	−9.181	−0.678	0.275	0.451
	13	8.83	−9.182	−0.698	0.274	0.449
	14	8.71	−9.135	−0.675	0.258	0.490
	15	9.20	−9.137	−0.681	0.258	0.490
	16	8.77	−9.139	−0.640	0.257	0.457
	17	8.67	−9.177	−0.677	0.274	0.462
	18	8.85	−9.187	−0.670	0.253	0.493
	19	9.00	−9.290	−0.621	0.257	0.525
	20	8.84	−9.139	−0.708	0.259	0.489
	21	8.79	−9.145	−0.675	0.257	0.476
	22	8.26	−9.160	−0.692	0.276	0.453
	23	8.65	−9.153	−0.661	0.295	0.474
	24	9.13	−9.150	−0.677	0.260	0.476
	25	8.70	−9.169	−0.655	0.267	0.462
	26	8.70	−9.156	−0.691	0.262	0.472
	27	9.00	−9.112	−0.693	0.247	0.490
	28	8.94	−9.177	−0.708	0.273	0.449

same side in Fig. 6. On the other hand, compounds with lower binding affinity values, on the right side, have more pronounced contributions from the other descriptors.

The selected descriptors, $\varepsilon_{\text{FERMO}}$, N^1 charge, $\sum_{(\text{FERMO})} c_i^2$, and ω' , were used to construct the dendrogram (see Fig. 8) that indicates that the compounds with lower binding affinity (with negative sign) are grouped together in the G1 cluster. The other molecules, with higher binding affinity values (with no sign), are gathered in the cluster denominated G2. These results agree with what we found through the PCA analysis.

3.2. Analysis of descriptors that influence the binding affinity values

Table 4 shows the calculated values for the four descriptors which were selected for further study, i.e., $\varepsilon_{\text{FERMO}}$, N^1 charge, $\sum_{(\text{FERMO})} c_i^2$ and ω' for the 28 compounds. The pK_i values allow a neat distinction between the two groups, I and II (see Table 4).

Table 4 also confirms that the compounds with higher pK_i values, belonging to group II, have $\varepsilon_{\text{FERMO}}$ values equal to −9.292 eV or higher. Compounds with lower binding affinity, constituents of group I, have values lower or equal to −9.290 eV. On this basis, it is suggested that the molecules with higher nucleophilic character tend to have higher binding affinity values.

The values of electrophilicity (ω'), also shown in Table 4, were clearly different for groups I and II. Indeed, group II shows values between 0.247 and 0.295 eV, whereas for group I, values vary from 0.431 to 0.468 eV. This result suggests that the lower the tendency of the molecules to attract electrons, the greater the binding affinity of the H_3 receptor.

As for the electronic density values ($\sum_{(\text{FERMO})} c_i^2$) in Table 4, there is no apparent difference between groups I and II. Perhaps the correlation between pK_i and $\sum_{(\text{FERMO})} c_i^2$ might be better understood by the regression equation obtained using the PLS method (see Refs. [37–39]). This approach led to Eq. (1), as we discuss in Section 3.3 below. Similar considerations may apply to the

performance of the N^1 charge values. Indeed, the use of both descriptors, $\sum_{(\text{FERMO})} c_i^2$ and N^1 , seems to be justified through the statistical validation of Eq. (1).

3.3. PLS regression equation

Employing three principal components for the PLS methodology [37–39] with 23 compounds (1–3, 6, 8–10, 12–20, 22–28), and validated through a leave-one-out cross-validation procedure, the external validation set (4, 5, 7, 11, 21), we arrive at Eq. (1) employing the four descriptors previously selected:

$$pK_i = 2.565(\varepsilon_{\text{FERMO}}) - 4.510(N^1) + 9.016 \left(\sum_{(\text{FERMO})} c_i^2 \right) - 5.867(\omega') + 26.571 \quad (1)$$

The statistical validity of this equation may be assessed by the values of the parameters R^2 , 0.927, and Q^2 , 0.880, as shown in Table 5. Considering these values, it appears that Eq. (1) explains 92.7% of the variance of the pK_i values and predicts 88.0% of the pK_i values. In addition, the correlation has a standard error validation close to zero (0.141) and a F Fisher value of 80.11. The differences between the experimental binding affinities and calculated values were relatively low, except for molecules 5 and 6 for which the

Table 5

Experimental and calculated binding affinities using the PLS regression equation.

Compound	$pK_{i(\text{experimental})}^a$	$pK_{i(\text{this work})}$	$\Delta (pK_{i(\text{experimental})} - pK_{i(\text{this work})})^b$
1	5.37	5.49	−0.12
2	7.09	7.05	0.04
3	6.97	6.65	0.32
4 ^c	7.55	6.97	0.58
5 ^c	6.12	7.05	−0.93
6	7.82	7.22	0.60
7 ^c	7.18	7.42	−0.24
8	7.89	7.72	0.17
9	7.49	7.85	−0.36
10	5.27	5.86	−0.59
11 ^c	8.52	8.92	−0.40
12	8.91	8.53	0.38
13	8.83	8.60	0.23
14	8.71	9.09	−0.38
15	9.20	9.11	0.09
16	8.77	8.62	0.15
17	8.67	8.64	0.03
18	8.85	8.98	−0.13
19	9.00	8.76	0.24
20	8.84	9.21	−0.37
21 ^c	8.79	8.94	−0.15
22	8.26	8.66	−0.40
23	8.65	8.62	0.03
24	9.13	8.92	0.21
25	8.70	8.60	0.10
26	8.70	8.92	−0.22
27	9.00	9.29	−0.29
28	8.94	8.67	0.27
Statistical parameters			Values
R^{2d}			0.927
Q^{2e}			0.880
SEP ^f			0.141
F^g			80.11
PCs ^h			3

^a Experimental pK_i values from Ref. [11].

^b Difference between experimental and calculated pK_i values in this work.

^c Samples for the external validation set.

^d Correlation coefficient from prediction.

^e Correlation coefficient from validation.

^f Standard error of validation.

^g The statistical Fisher test.

^h Number of principal components.

deviations were -0.93 and 0.6 , respectively; for all the other compounds the differences were lower than 0.6 . It thus seems valid to expect that Eq. (1) has statistical significance and potential to be used as a suitable regression model to interpret the dependence of the binding affinity with the chosen properties, and predict pK_i values with a satisfactory level of reliability.

4. Conclusions

For the present set of 28 molecules the FERMO energies seem to behave more appropriately for the description of binding affinities to H_3 histamine receptors than HOMO energies. In addition, this result suggests that the FERMO energy is a relevant descriptor to be taken into account in quantitative structure–activity relationship studies.

Considering both structural and quantum chemical factors, we may expect that new molecules with binding affinities values surpassing the set studied by Dvorak et al. [11] would benefit from the following factors: a chemical structure similar to molecules of group II, an electron donor group bound to N^1 , high values of $\varepsilon_{\text{FERMO}}$ and $\sum(\text{FERMO})\phi_i^2$, and low values of ω' .

We were able to confirm that four electronic descriptors were sufficient and appropriate for the classification of 28 molecules into groups of low and high binding affinity values, and to produce a reasonable prediction of pK_i values through a PLS regression equation.

From the calculated $\varepsilon_{\text{FERMO}}$ and ω' values shown in Table 4 for the 28 antihistamine compounds studied, we suggest that these compounds can be classified as electron donating compounds and have a great probability of interacting through a charge transfer process with the H_3 histamine receptor.

Acknowledgement

The authors acknowledge financial support from the Brazilian Agencies CAPES, CNPq, and FAPESP.

References

- [1] J.M. Arrang, M. Garbarg, J.C. Schwartz, Auto-inhibition of brain histamine release mediated by a novel class H_3 of histamine receptor, *Nature* 302 (1983) 832–837.
- [2] M.I. Martinez-Mir, H. Pollard, J. Moreau, J.M. Arrang, M. Ruat, E. Traiffort, J.C. Schwartz, J.M. Palacios, Three histamine receptors (H_1 , H_2 and H_3) visualized in the brain of human and non-human primates, *Brain Res.* 526 (1990) 322–327.
- [3] H. Haas, P. Panula, The role of histamine and the tuberomammillary nucleus in the nervous system, *Nat. Rev. Neurosci.* 4 (2003) 121–130.
- [4] J.M. Arrang, M. Garbarg, J.C. Schwartz, Autoregulation of histamine release in brain by presynaptic H_3 receptors, *Neuroscience* 15 (1985) 553–562.
- [5] J.M. Arrang, M. Garbarg, J.C. Schwartz, Autoinhibition of histamine synthesis mediated by presynaptic H_3 -receptors, *Neuroscience* 23 (1987) 149–157.
- [6] E. Schlicker, M. Kathmann, Modulation of in vitro neurotransmission in the CNS and in the retina via H_3 heteroreceptors, in: R. Leurs, H. Timmerman (Eds.), *The Histamine H_3 Receptor: A Target for New Drugs*, Elsevier, Amsterdam, 1998, pp. 13–26.
- [7] C.F. Wilkinson, K. Hetnarski, G.P. Cantwell, F.J.D. Carlo, Structure–activity relationships in the effects of 1-alkylimidazoles on microsomal oxidation in vitro and in vivo, *Biochem. Pharmacol.* 23 (1974) 2377–2386.
- [8] J.R. Halpert, Structural basis of selective cytochrome P450 inhibition, *Annu. Rev. Pharmacol. Toxicol.* 35 (1995) 29–53.
- [9] S. Celanire, M. Wijnmans, P. Talagaa, R. Leurs, I.J.P. De Esch, Histamine H_3 receptor antagonists reach out for the clinic, *Drug Discov. Today* 10 (2005) 1613–1627.
- [10] A.J. Barbier, C. Berridge, C. Dugovic, A.D. Laposky, S.J. Wilson, J. Boggs, L. Aluisio, B. Lord, C. Mazur, C.M. Pudiak, X. Langlois, W. Xiao, R. Apodaca, N.I. Carruthers, T.W. Lovenberg, Acute wake-promoting actions of JNJ-5207852, a novel, diamine-based H_3 antagonist, *Br. J. Pharmacol.* 143 (2004) 649–661.
- [11] C.A. Dvorak, R. Apodaca, A.J. Barbier, C.W. Berridge, S.J. Wilson, J.D. Boggs, W. Xiao, T.W. Lovenberg, N.I. Carruthers, 4-Phenoxypiperidines: potent, conformationally restrict, non-imidazole histamine H_3 antagonist, *J. Med. Chem.* 48 (2005) 2229–2238.
- [12] R.R. Da Silva, T.C. Ramalho, J.M. Santos, J.D. Figueroa-Villar, On the limits of highest-occupied molecular orbital driven reactions: the frontier effective-for-reaction molecular orbital concept, *J. Phys. Chem. A* 110 (2006) 1031–1040.
- [13] K. Fukui, The role of frontier orbitals in chemical reactions (Nobel Lecture), *Angew. Chem. Int. Ed.* 21 (1982) 801–809.
- [14] H. Fujimoto, Y. Mizutani, K. Iwase, An aspect of substituents and peripheral structures in chemical reactivities of molecules, *J. Phys. Chem.* 90 (1986) 2768–2772.
- [15] H. Fujimoto, Paired interacting orbitals: a way of looking at chemical interactions, *Acc. Chem. Res.* 20 (1987) 448–453.
- [16] K. Omoto, H. Fujimoto, Electron-donating and -accepting strength of enoxysilanes and allylsilanes in the reaction with aldehydes, *J. Am. Chem. Soc.* 119 (1997) 5366–5372.
- [17] H. Hirao, T. Ohwada, Theoretical study of reactivities in electrophilic aromatic substitution reactions: reactive hybrid orbital analysis, *J. Phys. Chem. A* 107 (2003) 2875–2881.
- [18] T. Ohwada, H. Hirao, A. Ogawa, Theoretical analysis of Lewis basicity based on local electron-donating ability. Origin of basic strength of cyclic amines, *J. Org. Chem.* 69 (2004) 7486–7494.
- [19] S. Nakamura, H. Hirao, T. Ohwada, Rationale for the acidity of meltdrum's acid. Consistent relation of C–H acidities to the properties of localized reactive orbital, *J. Org. Chem.* 69 (2004) 4309–4316.
- [20] H. Hirao, T. Ohwada, Theoretical revisit of regioselectivities of diels-alder reactions: orbital-based reevaluation of multicentered reactivity in terms of reactive hybrid orbitals, *J. Phys. Chem. A* 109 (2005) 816–824.
- [21] P. Chen, K. Fujisawa, E.I. Solomon, Spectroscopic and theoretical studies of mononuclear copper(II) alkyl- and hydroperoxo complexes: electronic structure contributions to reactivity, *J. Am. Chem. Soc.* 122 (2000) 10177–10193.
- [22] HyperChem, version 6.03, Hyper cube, Inc., Florida, USA, 2000.
- [23] C.C.J. Roothaan, New developments in molecular orbital theory, *Rev. Modern Phys.* 23 (1951) 69–89.
- [24] M.J. Frisch, G.W. Trucks, H.B. Schlegel, G.E. Scuseria, M.A. Robb, J.R. Cheeseman, J.A. Montgomery Jr., T. Vreven, K.N. Kudin, J.C. Burant, J.M. Millam, S.S. Iyengar, J. Tomasi, V. Barone, B. Mennucci, M. Cossi, G. Scalmani, N. Rega, G.A. Petersson, H. Nakatsuji, M. Hada, M. Ehara, K. Toyota, R. Fukuda, J. Hasegawa, M. Ishida, T. Nakajima, Y. Honda, O. Kitao, H. Nakai, M. Klene, X. Li, J.E. Knox, H.P. Hratchian, J.B. Cross, C. Adamo, J. Jaramillo, R. Gomperts, R.E. Stratmann, O. Yazyev, A.J. Austin, R. Cammi, C. Pomelli, J.W. Ochterski, P.Y. Ayala, K. Morokuma, G.A. Voth, P. Salvador, J.J. Dannenberg, V.G. Zakrzewski, S. Dapprich, A.D. Daniels, M.C. Strain, O. Farkas, D.K. Malick, A.D. Rabuck, K. Raghavachari, J.B. Foresman, J.V. Ortiz, Q. Cui, A.G. Baboul, S. Clifford, J. Cioslowski, B.B. Stefanov, G. Liu, A. Liashenko, P. Piskorz, I. Komaromi, R.L. Martin, D.J. Fox, T. Keith, M.A. Al-Laham, C.Y. Peng, A. Nanayakkara, M. Challacombe, P.M.W. Gill, B. Johnson, W. Chen, M.W. Wong, C. Gonzalez, J.A. Pople, Gaussian 03, Revision C.02, Gaussian, Inc., Wallingford, CT, 2004.
- [25] Minitab Statistical Software Package, Release 14.1 for Windows, Minitab, Inc., USA, 2003.
- [26] C.M. Breneman, K.B. Wiberg, Determining atom-centered monopoles from molecular electrostatic potentials. The need for high sampling density in formamide conformational analysis, *J. Comp. Chem.* 11 (1990) 361–373.
- [27] R. Apodaca, C.A. Dvorak, W. Xiao, A.J. Barbier, J.D. Boggs, S.J. Wilson, T.W. Lovenberg, N.I. Carruthers, A new class of diamine-based human histamine H_3 receptor antagonists: 4-(aminoalkoxy)benzylamines, *J. Med. Chem.* 46 (2003) 3938–3944.
- [28] H. Kurtz, D. Dudis, Quantum mechanical methods for predicting nonlinear optical properties, in: K. Lipkowitz, D. Boyd (Eds.), *Reviews in Computational Chemistry*, Wiley-VCH, New York, 1998, pp. 241–279.
- [29] K.M. Honório, L.G. Freitas, M. Trsic, A.B.F. Da Silva, A quantum chemical study on the psychoactivity of cannabinoid compounds, *J. Mol. Struct.: Theochem.* 538 (2001) 99–106.
- [30] B.W. Clare, Frontier orbital energies in quantitative structure–activity relationships: a comparison of quantum chemical methods, *Theor. Chim. Acta.* 87 (1994) 415–430.
- [31] T.A. Nguyen, *Frontier Orbitals: A Practical Manual*, Chichester, England, 2007.
- [32] S. Subramanian, M.M.C. Ferreira, M. Trsic, A structure–activity relationship study of lapachol and some derivatives of 1,4-naphthoquinones against carcinosarcoma walker 256, *Struct. Chem.* 9 (1998) 47–57.
- [33] R.G. Pearson, Absolute electronegativity and hardness correlated with molecular orbital theory, *Proc. Natl. Acad. Sci. U.S.A.* 83 (1986) 8440–8441.
- [34] R.G. Parr, L.V. Szentpály, S. Liu, Electrophilicity index, *J. Am. Chem. Soc.* 121 (1999) 1922–1924.
- [35] R.R. Da Silva, J.M. Santos, T.C. Ramalho, J.D. Figueroa-Villar, Concerning the FERMO concept and Pearson's hard and soft acid–base principle, *J. Braz. Chem. Soc.* 17 (2006) 223–226.
- [36] G.E.P. Box, W.G. Hunter, J.S. Hunter, *Statistics for Experimenters: An Introduction to Design, Data Analysis and Model Building*, Wiley, New York, 1978.
- [37] K.R. Beebe, R.J. Pell, M.B. Seasholtz, *Chemometrics: A Practical Guide*, John Wiley & Sons, New York, 1998.
- [38] P. Geladi, B.R. Kowalski, Partial least-squares regression: a tutorial, *Anal. Chim. Acta* 185 (1986) 1–17.
- [39] M.M.C. Ferreira, A.M. Antunes, M.S. Melgo, P.L.O. Volpe, Chemometrics I: multivariate calibration, a tutorial, *Quim. Nova* 22 (1999) 724–731.